

On the conformational structure of a stiff homopolymer

Yu.A. Kuznetsov, E.G. Timoshenko*

*Theory and Computation Group, Department of Chemistry,
University College Dublin, Belfield, Dublin 4, Ireland
(February 6, 2018)*

In this paper we complete the study of the phase diagram and conformational states of a stiff homopolymer. It is known that folding of a sufficiently stiff chain results in formation of a torus. We find that the phase diagram obtained from the Gaussian variational treatment actually contains not one, but several distinct toroidal states distinguished by the winding number. Such states are separated by first order transition curves terminating in critical points at low values of the stiffness. These findings are further supported by off-lattice Monte Carlo simulation. Moreover, the simulation shows that the kinetics of folding of a stiff chain passes through various metastable states corresponding to hairpin conformations with abrupt U-turns.

PACS numbers: 36.20.-r, 36.20.E, 87.15.B

I. INTRODUCTION

Conformational transitions of semi-flexible polymers have been of considerable interest for analytical studies^{1–5} and computer simulations^{6–8} recently. Polymers can possess different degree of flexibility and their persistent length λ is one of the key parameters that determine the conformation^{9,10}. For example, for polystyrene $\lambda \simeq 1.4$ nm, which corresponds to about 5 chain bonds, whereas for the double helix DNA $\lambda \simeq 50$ nm, i.e. about 150 base pairs.

The equilibrium^{9,10} and kinetics of folding^{11–13} of a flexible homopolymer ($\lambda = 0$) are relatively well understood at present. It is believed that in a wide range of interaction parameters the equilibrium collapse transition is continuous. As the persistent length increases the extended coil becomes larger with the swelling exponent changing smoothly from that of the Flory coil $\nu = 3/5$ to that of a rigid rod $\nu = 1$. The collapse transition of a semi-flexible homopolymer on going from the good to the poor solvent regime remains continuous at first, but starting from some critical value of λ becomes discontinuous^{9,3}. Such a change of the nature of the transition actually reflects a profound restructuring of the collapsed globule. Thus, instead of forming a nearly spherical liquid-like globule a sufficiently stiff chain has no point of easy bending so that it wraps around itself forming a *torus*. Such structures have been observed a number of times experimentally for DNA molecules¹⁴ and were studied theoretically from different points of view¹⁵ starting from a pioneering work¹⁶.

In works Refs. 5,3 it has been noted that for a given degree of polymerisation the toroidal conformation exists in a region starting from some value of stiffness λ and in a limited interval of the solvent quality. In Ref. 3 based on the Gaussian self-consistent (GSC) method we have studied the equilibrium phase diagram and kinetics of conformational transitions after various quenches. Importantly, both transitions coil-to-torus and torus-to-globule are discontinuous, and thus there are associated regions of metastability. This results in a rather complex kinetic picture of expansion or folding, essentially dependent on the quench depth. In that work we have also mentioned that there seemed to be some additional minima of the free energy, the study of which has been deferred until the current paper.

In Ref. 17 we have shown that at equilibrium the GSC treatment precisely reduces to the Gibbs-Bogoliubov variational method with a generic quadratic trial Hamiltonian. However, in the extended variational space care should be taken while finding the true free energy minima as these seem to be sensitive to the limitations of the underlying polymer model. The current model with a virial-type expansion is believed to have problems at high densities. Thus we shall re-examine the phase diagram of a semi-flexible chain here in a more systematic and accurate manner.

Despite a relative ease for analytical theories to obtain the toroidal conformation, computer simulations have been less successful so far. In Ref. 7 an attempt was made to include the bending energy into Monte Carlo simulation in a lattice model of Ref. 18. Although a number of metastable states corresponding to conformations with hairpin and crystalline conformations were observed, the true equilibrium state corresponding to the torus was not possible to obtain. These difficulties are due to a number of circumstances. First, a toroidal conformation appears only for sufficiently long and stiff chains. However, the relaxation times for these become enormous and the equilibrium state is

*Corresponding author. Internet: <http://darkstar.ucd.ie>; E-mail: Edward.Timoshenko@ucd.ie

hard to reach during a limited simulation time. Second, the lattice itself introduces a number of unfortunate artefacts. This is because the rotational symmetry is broken, so that the chain segments can lie only along a number of allowed directions, and thus weak bendings are simply impossible. So, the chain forms conformations with long straight sections which then possess a U-turn, resembling a hairpin. Such abrupt turns, however, produce a considerable energetic penalty, so that the corresponding states have a higher free energy than the true minimum. Depending on the particular type of the lattice model used the true minimum may still be a mis-shapen torus, or if the smallest and only bendings are 90 degrees, one would expect instead a kind of a solid-like crystalline ordering^{19,6}. Even though a kind of torus may be possible in the model with links along 2-D and 3-D diagonals¹⁸, such a state would be extremely hard to reach due to the lack of collective moves and a huge number of metastable minima in which the system would tend to be trapped. Interestingly, in a recent paper Ref. 8 a simulation in the bond fluctuation model, which is intermediate between the lattice and continuous space models, has exhibited a toroidal, though imperfect, structure (see e.g. Fig. 7).

One attractive possibility is to use Langevin or Monte Carlo simulations in continuous space instead, although this would require much longer computations. Here we shall use a fairly standard Monte Carlo off-lattice technique for a ring homopolymer chain.

Thus, the main objective of this work is by using both the Gaussian variational and Monte Carlo techniques to obtain a more accurate phase diagram of the homopolymer in terms of the stiffness and the solvent quality and to elucidate the conformational structure of corresponding thermodynamically stable as well as possible metastable states.

II. TECHNIQUES

A. Gaussian variational method

The Gaussian variational method is based on minimising the Gibbs–Bogoliubov trial free energy, $\mathcal{A} \equiv \mathcal{E} - T\mathcal{S}$, with respect to the full set of variational parameters. Here these are the mean-squared distances, $D_{mm'} \equiv (1/3)\langle(\mathbf{X}_m - \mathbf{X}_{m'})^2\rangle$, between monomers number m and m' ($m, m' = 0, \dots, N-1$, where N is the degree of polymerisation). For a ring homopolymer the matrix $D_{mm'}$ is translationally invariant along the chain: $D_{mm'} \equiv D_k$, where $k = |m - m'|$.

Using the de Gennes–des Cloizeaux–Edwards bead-and-spring model^{9,10} of the homopolymer with the volume interactions represented by the virial-type expansion, one can obtain the following entropic and the energetic contributions^{3,17},

$$\mathcal{S} = \frac{3k_B}{2} \sum_{q=1}^{N-1} \log \mathcal{F}_q, \quad \mathcal{F}_q = -\frac{1}{2N} \sum_{k=1}^{N-1} \cos\left(\frac{2\pi kq}{N}\right) D_k, \quad R_g^2 \equiv \sum_{q=1}^{N-1} \mathcal{F}_q, \quad (1)$$

$$\begin{aligned} \mathcal{E} = & \frac{3N k_B T}{2l^2} D_1 + \frac{3N k_B T \lambda}{2l^3} (4D_1 - D_2) + \frac{u^{(2)} N}{(2\pi)^{3/2}} \sum_{k=1}^{N-1} D_k^{-3/2} + \frac{3u^{(3)} N}{(2\pi)^3} \sum_{k=1}^{N-1} D_k^{-3} \\ & + \frac{u^{(3)} N}{(2\pi)^3} \sum_{k_1 \neq k_2=1}^{N-1} \left(\frac{1}{2} (D_{k_1} D_{k_2} + D_{k_1} D_{k_1-k_2} + D_{k_2} D_{k_1-k_2}) - \frac{1}{4} (D_{k_1}^2 + D_{k_2}^2 + D_{k_1-k_2}^2) \right)^{-3/2}, \end{aligned} \quad (2)$$

where we have also introduced the normal modes \mathcal{F}_q and the mean squared radius of gyration of the chain R_g^2 .

Analogously to Eqs. (8-11) of Ref. 3 the first term in Eq. (2) is the elastic energy of springs and the second term is the bending energy, with l and λ being the statistical and the persistent lengths of the chain respectively. Note that these formulas correspond precisely to the Kratky–Porod model of taking the stiffness into account by adding the integral along the chain of the squared curvature^{20,21}.

In Refs. 17,22 we have discussed that the application of a virial-type expansion is flawed for the dense globular state. Namely, the model with the two- and three-body terms²³ in the variational treatment is found to possess a number of pathological infinitely deep free energy minima. This implies that for a sufficiently high density the three-body term is unable to cope with the increasingly strong two-body attraction. Introduction of a thermodynamically subdominant term such as the 4th term in Eq. (2), \mathcal{E}_{si} (see Appendix for more details), or the so-called ‘thickness’ term in Ref. 24, fixes the problem, and is also shown to produce a negligibly weak correction in the repulsive and ideal coil regimes. Although attempts to derive such a term from the perturbation and renormalisation theory have been made (as e.g. in the latter work), these partial fixes are fundamentally inconsistent. Having convinced ourselves that for the purpose of the current work the results from such a theory are in satisfactory agreement with the numerical experiment, we shall accept this procedure here and bear in mind its limitations. Hopefully, a new non-Gaussian theory under

development by one of the authors²⁵ may address this problem. It fundamentally deals with true intermolecular interaction potentials instead of ill-defined virial expansions, something which the Gaussian variational theory can not avoid since the energy averaged over a Gaussian trial distribution diverges for any singular potential involving a hard-core part.

B. Off-Lattice Monte Carlo Simulation

Since the lattice Monte Carlo model^{18,7} is not suitable for study of the effects of chain stiffness for several reasons, we have carried out simulation in continuous space instead. The disadvantages of the lattice model include the rotational anisotropy and tendency for condensed phases to form some kind of crystalline structures on the lattice¹⁹. Thus, to produce toroidal states on a lattice for comparatively short polymer chains is rather difficult. Another disadvantage of the lattice model is that the persistence of the polymer chain reduces dramatically the acceptance ratio of the local monomer moves and, thus, other more sophisticated types of moves such as shifts and rotations of chain segments as a whole are needed.

The model is implemented for a single homopolymer consisting of N monomers connected by springs in a ring, which additionally interact with each other via a pair-wise short ranged spherically symmetric potential,

$$H = \frac{k_B T}{2l^2} \sum_m (\mathbf{X}_m - \mathbf{X}_{m-1})^2 + \frac{k_B T \lambda}{2l^3} \sum_m (\mathbf{X}_{m+1} + \mathbf{X}_{m-1} - 2\mathbf{X}_m)^2 + \frac{1}{2} \sum_{m \neq m'} V(|\mathbf{X}_m - \mathbf{X}_{m'}|). \quad (3)$$

Unlike the GSC theory, where one has to introduce a virial-type expansion representing the pair-wise potential, here we use the two-body interaction potential explicitly,

$$V(r) = \begin{cases} +\infty & \text{for } r < d \\ V_0 \left(\left(\frac{d}{r}\right)^{12} - \left(\frac{d}{r}\right)^6 \right) & \text{for } r > d \end{cases}. \quad (4)$$

Thus, monomers are represented by hard spheres of the diameter d , with a weak short ranged Lennard-Jones attraction of characteristic strength V_0 . During simulation we change the strength of the two-body attraction V_0 , which can be viewed as basically the “inverse temperature”, rather than changing the temperature T itself.

The Monte Carlo updates scheme is based on the Metropolis algorithm with local monomer moves. The new coordinate of a monomer can be sought as, $q^{new} = q^{old} + r_\Delta$, where q stands for x , y and z spatial projections and r_Δ is a random number uniformly distributed in the interval $[-\Delta, \Delta]$. Here Δ is some additional parameter of the Monte Carlo scheme, which, in a sense, characterises the timescale involved in the Monte Carlo sweep (MCS), the latter being defined as N attempted Monte Carlo steps.

In both models we work in the system of units such that $l = 1$ and $k_B T = 1$. Additionally we fix the third virial coefficient in the variational method, $u^{(3)} = 10$, and the hard-core diameter, $d = 1$, in Eq. (4).

III. EQUILIBRIUM PHASE DIAGRAM FROM THE VARIATIONAL METHOD

First, let us consider the system behaviour upon a quasistatic change of the interaction parameters. In Fig. 1 we present the plot of the mean squared radius of gyration, R_g^2 , versus the second virial coefficient, $u^{(2)}$, at a fixed stiffness parameter, λ . The regime of repulsion and comparatively weak attraction in the right-hand-side of the figure corresponds to the extended coil conformation of the polymer with a large radius of gyration scaling as $R_g \sim N^{\nu_{coil}}$, where the exponent ν_{coil} is close to the Flory value $\nu_F = 3/5$ for a flexible chain, $\lambda = 0$, becomes a rigid rod exponent $\nu_{rod} = 1$ for a very stiff chain, with a cross-over in between. Since increasing the stiffness leads to a stronger effective repulsion between monomers, the extended phase expands to the region of the negative second virial coefficient for higher values of the stiffness parameter.

For comparatively small values of λ the plot of the radius of gyration (solid line and diamonds in Fig. 1) is quite similar to that of the flexible homopolymer at the equilibrium coil-to-globule transition (see e.g. Fig. 1 in Ref. 12), which is second order. However, at higher values of the stiffness parameter the collapse transition becomes first order²⁶. In this case, after the system has been quasistatically quenched to the region of a higher monomer attraction (line denoted by pluses in Fig. 1), the local minimum corresponding to the coil suddenly disappears becoming an inflexion point somewhere in the interval, $-23 < u^{(2)} < -22$, and the system passes to another free energy minimum with a much smaller value of the radius of gyration. Similarly, upon changing $u^{(2)}$ quasistatically towards monomer repulsion (line denoted by quadrangles in Fig. 1), the free energy minimum disappears in the interval $-12 < u^{(2)} < -11$, and

the system transforms into the coil state. If at least two minima of the free energy can coexist in some interval of the interaction parameters, the transition point is defined by the condition that the current minimum of the free energy \mathcal{A} becomes the deepest one. Observables such as the mean energy, \mathcal{E} , the mean squared radius of gyration, R_g^2 , and the mean squared distances between monomers, $D_{mm'}$, experience a discontinuous jump at such a transition.

It is important to note that upon a quasistatic change of the second virial coefficient towards repulsion (line denoted by quadrangles in Fig. 1) the mean squared radius of gyration increases in a three-step-like fashion before the homopolymer expands to the coil. This is a manifestation of some additional condensed phases, which we have denoted by labels (T5), (T6) and (T7). To understand the distinction between these phases and the conventional globule let us compare the monomer–monomer mean squared distances, D_k , in these phases. These are exhibited in Figs. 2a, b. As we have discussed earlier^{11,12} for the state of the extended coil this function monotonically increases on the half-period of the chain. The situation remains similar for the coil of a stiff homopolymer (line denoted by diamonds in Fig. 2a).

However, the function D_k is more sensitive to the stiffness in the state of the globule, especially at small values of the chain index k (compare the line denoted by pluses with the solid line in Fig. 2a). At small values of k the function is nearly parabolic, $D_k \sim |k|^2$, i.e. the chain represents almost a rigid rod, reaching a maximum at some value of the chain index k^* . In some intermediate range of the chain index, $0 < k \lesssim 6k^*$, one can see about 2-3 oscillations in the function D_k , with the amplitude decreasing quickly to stabilise at some level. At higher values of the chain index towards half of the chain the function remains constant. Thus, we can conclude that for small chain distances the structure of the globule of a fairly stiff polymer is quite different from that of the flexible chain. This is easy to understand. For a semi-flexible polymer chain segments in the globule are locally straightened on a characteristic scale related to λ . As long as this scale is considerably smaller than the globule size the shape of D_k remains flat as for the flexible chain. When this scale becomes comparable to the globule size, a few oscillations appear in the mean squared distances.

Transition from the conventional globule to the phase labelled as (T7) is accompanied by a spectacular change of the function D_k (see line denoted by quadrangles in Fig. 2b). In this phase the function strongly oscillates with the amplitude decreasing rather slowly towards half of the chain. The ratio of the value of D_k in a maximum to that in a minimum is about 5-6 near the middle of the chain. The designation of the phases is done according to the number of oscillations: in phase (T7) there are 7 oscillations, in phase (T6) there are 6 oscillations (line denoted by pluses in Fig. 2b), and in phase (T5) there are 5 oscillations (line denoted by diamonds). We also note that the smaller the number of oscillations the higher is the ratio of the value of D_k in a maximum to that in a minimum.

We claim that the phases (Tn) correspond to the toroidal conformation with the number of windings $\mathcal{N}_w = n$. The chain index k^* , where the function D_k reaches its first maximum, is equal to the number of monomers forming half-period of the first winding starting from the zeroth monomer. Therefore, $D_{max} = D_{k^*}$ may be interpreted roughly as the mean squared *external* diameter of the torus. By moving from the monomer number k^* to $2k^*$ the first winding is completed. However, because of the excluded volume interaction the chain cannot return to the same coordinate, giving rise in the average to the value $D_{min} = D_{2k^*}$, which may be considered as the mean squared *internal* diameter of the torus. The winding number \mathcal{N}_w is thus precisely the number of oscillations in D_k . The physical reason for a torus is clear — a persistent chain has no desire to bend, so it tends to have as large a radius of curvature as possible, however, two-body attraction tends to keep quite close packing of the chain.

A quasistatic increase of the repulsion (see line denoted by quadrangles in Fig. 1) results in transformation of the conventional globule to the toroidal globule with $\mathcal{N}_w = 7$ windings in the interval, $-27 < u^{(2)} < -26$. This is a rather weak discontinuous transition. It occurs when the characteristic scale of straightened segments reaches the size of the globule, and a hole in the centre of the globule is formed. Transitions between various toroidal states are also first order, but much stronger since they are accompanied by a global restructuring of the polymer conformation.

In Fig. 3 we present the plots of the mean squared radius of gyration, R_g^2 , upon a quasistatic change of the stiffness parameter λ for different fixed negative values of the second virial coefficient, $u^{(2)}$, corresponding to the globule at $\lambda = 0$. The radius of gyration increases monotonically during this change. The most significant changes occur in the region of rather small stiffness parameter, $0 < \lambda < 1/2$, and in the region where the conventional globule transforms to the toroidal state. The second change is associated with a weak first order transition. Note that the final toroidal state depends on the value of the second virial coefficient. At a weaker attraction the globule is transformed to a toroidal state with a smaller winding number. However, the transition from the coil to the toroidal phases upon a quasistatic change of $u^{(2)}$ (line denoted by pluses in Fig. 1) is quite difficult due to a large potential barrier, which makes the coil a metastable state in a large region of the phase diagram.

In Fig. 4 we present the resulting phase diagram of the stiff homopolymer in terms of the second virial coefficient, $u^{(2)}$, and the stiffness parameter, λ . It contains phases of the coil, where monomer attraction is insufficient to form compact states, the globule in the region of either a low stiffness or a strong monomer attraction, and a number of toroidal phases characterised by distinct winding number \mathcal{N}_w . As we have already discussed above the collapse

transition changes its behaviour from continuous to discontinuous starting from some value of the stiffness. The globule of a semi-flexible polymer is different in the local structure from that of the flexible homopolymer, although global scaling characteristics are the same for both cases. The toroidal phases lie in the intermediate region in $u^{(2)}$ starting from some critical values of the stiffness parameter. Some of such states with $\mathcal{N}_w = 2, 3, 4$ are always metastable, while some with $\mathcal{N}_w = 5, 6, 7$ can become thermodynamically stable.

For a large fixed value of the stiffness parameter the number of toroidal phases increases approximately linearly with the degree of polymerisation, N . For example, the maximal winding numbers at $\lambda = 25$ for polymers with the degree of polymerisation $N = 50, 100, 150$ and 200 are equal to: $\mathcal{N}_w = 4, 7, 10$ and 13 respectively.

IV. RESULTS FROM MONTE CARLO SIMULATION

In series of pictures in Fig. 5 we exhibit typical conformations in various phases from the off-lattice Monte Carlo simulation. Fig. 5a corresponds to the extended conformation, which for large values of the stiffness parameter takes a form close to a ring. In Fig. 5b we draw the backbone of a typical globular conformation for the values of the stiffness parameter not large enough to form a toroidal state. The globule structure here is quite different from that of a flexible homopolymer in Fig. 5c. One can see that it consists of entangled loops of a radius close to the size of the globule. The function of the mean squared distances between monomers here possesses a typical form presented by pluses in Fig. 2a with significant oscillations on small chain distances, which quickly saturate due to varying number of monomers in each loop. We should also note that the globule of a stiff homopolymer is not quite spherical, but rather reminds an ellipsoid, either flattened or elongated. Thus, we avoid calling it “spherical globule” as we did in Ref. 3. Increasing the stiffness parameter transforms such a globule to the toroidal conformation exhibited in Fig. 5d.

It is important to note that to produce the globule state as in Fig. 5b, or the toroidal state as in Fig. 5d, in a Monte Carlo simulation it is much easier to bring the system first to the globule of the flexible homopolymer (Fig. 5c), and then to increase the stiffness parameter quasistatically. If instead we change V_0 quasistatically at a fixed sufficiently large λ reaching the equilibrium would be difficult. First, as we have mentioned earlier, the region of the metastable coil is rather wide for large values of the stiffness. Second, the system may become trapped in a metastable state during such a process. Polymer conformation in these states have a typical form of a *hairpin* (see Fig. 6c). Here the chain folds a few times along a nearly straight line forming abrupt U-turns near the ends. However, these ends contribute more significantly to the bending energy than a uniform slow bending. Thus, such conformations possess a higher energy and hence are metastable.

Let us consider in more detail the kinetic process of pairpin formation after an instantaneous change of the two-body attraction, V_0 , starting from the ring-like conformation as in Fig. 5a. Due to the stiffness the initial ring conformation remains stable for some time. However, due to thermal fluctuations some distant parts of the chain would meet each other occasionally, so that the chain acquires a shape of the digit ‘8’ as in Fig. 6a. If monomers are attractive enough, parts of the chain would align along each other starting from the centre towards ends (see Fig. 6b). The process can repeat itself if the persistent length is shorter than half of the chain. Without performing quite sophisticated collective movements of the chain segments it is virtually impossible to proceed further towards the fully collapsed state. Snapshot in Fig. 6c corresponds to 10^7 MCSs and the system is still trapped in the same hairpin state.

In series of pictures in Fig. 7 we exhibit polymer conformations during kinetics of folding for a smaller value of the stiffness parameter, $\lambda = 5$. After a long evolution during which the ring remains practically unchanged some loops of a size comparable to the persistent length are formed (see Fig. 7a), which continue to grow by picking up the slack of the chain and thus forcing a few more loops to form. Then a kind of a star-like structure including a few hairpins is produced as in Fig. 7b. These hairpins fold onto each other producing a *sausage*-like object (see Fig. 7c). Further rather slow kinetic process involves refolding of the sausage which is accompanied by its broadening and shortening (see Fig. 7d). Thus, kinetics of folding leads to elongated sausage-like conformations, whereas a similar quasistatic change of the stiffness would tend to produce a flattened rather than elongated globule (see Fig. 5b).

Finally, let us note that the hairpin conformations have not been obtained by the GSC method neither at equilibrium, nor even as intermediate kinetic states, although they are present as local free energy minima. This is probably related to that in the Gaussian method the monomer-monomer correlation functions are represented by only one parameter characterising the mean squared distances. On the other hand, the lack of collective moves in the Monte Carlo scheme quite likely overestimates the stability of hairpin conformations as metastable or kinetically arrested states.

V. CONCLUSION AND DISCUSSION

In this paper we have completed the study of the phase diagram of a stiff homopolymer based on the Gaussian variational method and have also performed some equilibrium and kinetic Monte Carlo simulations in continuous space. Compared to the previous work Ref. 3 we have shown here that the region corresponding to the toroidal globule actually consists of a number of strips corresponding to tori with different *winding numbers*. The transition curves separating such states from each other, as well as from the coil and the spherical globule, all correspond to first order transitions and terminate in critical points. For a given sufficiently large degree of polymerisation N there exist a certain number of different toroidal states, which grows with N approximately linearly. The distinction between such toroidal states is clearly visible in the function of the mean squared distances between monomers, which shows precisely the number of oscillations equal to the winding number. The existence of the toroidal states has been also confirmed by off-lattice Monte Carlo simulation for the similar model of local stiffness. In addition, hairpin conformations with abrupt U-turns corresponding to metastable states have been observed. These also appear as nonequilibrium intermediaries during kinetics of folding.

We should emphasise that the results in the previous work Ref. 3 at sufficiently strong monomer attractions do suffer somewhat from the artefacts of the de Gennes–des Cloizeaux–Edwards bead-and-spring model based on the virial expansion. Here, by including the \mathcal{E}_{si} -term introduced in Ref. 17, we have managed to fix the problem at a practical level, although its fundamental resolution remains the matter of future work²⁵. The changes in the results are as follows. First, the region designated as ‘Torus’ in Fig. 1 of Ref. 3 expands and covers all of the region designated as ‘Spherical Globule’ there (i.e. curves III, III’, III’’ in Fig. 1 of Ref. 3 shift to the left of the axis $\lambda = 0$). Indeed, a slightly oscillating behaviour of D_k is only related to the existence of locally straightened sections of the chain, and does not necessarily correspond to a torus. Second, the metastable states which we called T’, T’’ and so on in Fig. 6 of Ref. 3 now become thermodynamically stable in some regions of the phase diagram in Fig. 4. Oscillations of the function D_k for the true toroidal states are much stronger (see Fig. 2b) and this function never reaches a steady level. Most importantly, there are a few distinct toroidal states of a ring polymer separated by first order transitions and distinguished by the winding number. Nevertheless, the main conclusion of Ref. 3 that the toroidal conformation exists in a triangularly shaped region of the phase diagram, remains valid. Most of the general conclusions about the stability of the toroidal conformation and kinetics of conformational changes of Ref. 3 remain unchanged too.

We would like to emphasise that the existence of the toroidal states is pretty much related to the choice of the bending energy as the square of the local curvature of the chain. Indeed, such a choice is natural for representing the persistent flexibility of polymers, which is due to rather small harmonic fluctuations in bending of the chain sections. This mechanism of flexibility is dominant for many helical or rather stiff chains such as DNA, for which the toroidal states have been observed experimentally¹⁴.

The rotational–isomeric flexibility is also very important for many polymers. Such polymer molecules exhibit flexibility due to rotation around carbon–carbon and other bonds, as the minima of the torsional potential corresponding to the *gauche* and *trans* configurations have the difference in their depth of about $k_B T$. For representing this mechanism of flexibility a model with discrete bending angles is more appropriate. Such models, however, possess crystalline solid-like states^{19,6} instead of toroidal ones. Such a difference in conformational states is genuine in our view and both types of structures are observable experimentally depending on the particular polymer system.

Another important prerequisite for obtaining a toroidal state even in a model with persistent flexibility mechanism is that the processes of inter-chain aggregation do not occur, otherwise more complicated self-assembled structures may be formed. For instance, aggregation of triple helix collagen molecules leads to self-assembly of various fibrils.

ACKNOWLEDGMENTS

The authors are grateful for most interesting discussions to Professor A.Yu. Grosberg and Professor K.A. Dawson, and also to Professor K. Binder and Dr A.V. Gorelov. One of us (E.G.T.) acknowledges the support of the Enterprise Ireland grants IC/1999/001 and SC/99/186.

APPENDIX: THE SELF-INTERACTION ENERGY TERM

Let us discuss in more detail the appearance of the last term, \mathcal{E}_{si} , in Eq. (2), which we call the self-interaction energy term. Such a term has been introduced in Ref. 17 for heteropolymers, for which the two-body interaction matrix, $u_{mm}^{(2)}$, is site dependent. Generally, one has to discard the singular terms with coinciding indices in the virial expansion as we have done in Eq. (2). It turns out, however, that the resulting free energy possesses some pathological

minima with singular free energy if at least one element of the matrix $u_{mm'}^{(2)}$ becomes negative. Indeed, let us consider the interactions of just three monomers under the condition that the mean squared distances from monomers '0' and '1' to '2' are equal to each other, $D_{0,2} = D_{1,2} = D$. These interactions produce the mean energy contribution,

$$\mathcal{E}_3 = \frac{u_{0,2}^{(2)} + u_{1,2}^{(2)}}{(2\pi D)^{3/2}} + \frac{1}{(2\pi D_{0,1})^{3/2}} \left(u_{0,1}^{(2)} + \frac{6u^{(3)}(2\pi)^{-3/2}}{(D - D_{0,1}/4)^{3/2}} \right) \quad (\text{A1})$$

If $u_{0,1}^{(2)} < 0$ and monomer '2' is placed away from monomers '0' and '1', $D > D_{0,1}/4 + (6u^{(3)}(2\pi)^{-3/2}/|u_{0,1}^{(2)}|)^{2/3}$, obviously, in the limit $D_{0,1} \rightarrow 0$ the mean energy possesses a singular minimum, $\mathcal{E}_3 \rightarrow -\infty$. As for the free energy, the logarithmic divergence of the entropy could not change the situation, thus $\mathcal{A} \rightarrow -\infty$ as well. One can also show that the inclusion of more monomers in the chain, or of higher than the three-body interactions, does not improve the situation, but produces more and more of such pathological solutions.

The problem can be quite easily remedied by using another prescription — replacing the terms with coinciding indices by the self-interaction terms^{17,22}. Namely, we should add the following term,

$$\mathcal{E}_{si} = c_3 u^{(3)} \sum_{m \neq m'} \left\langle \delta(\mathbf{X}_m - \mathbf{X}_{m'}) \right\rangle^2 = c_3 \frac{u^{(3)}}{(2\pi)^3} N \sum_k D_k^{-3}, \quad (\text{A2})$$

where $c_3 = 3$ is a combinatorial factor related to the three possible ways of having coinciding pairs of indices in a triple summation. Obviously, the higher negative power of D_k in Eq. (A2) compared to the two-body term in Eq. (2) prevents one monomer from falling onto another.

Interestingly enough, this problem is hidden for a ring homopolymer. Indeed, due to the inverse symmetry²⁸, we have the property that for any indices m, m' the following mean squared distances are equal: $D_{m,m'} = D_{m,2m-m'} = D_{2m'-m,m'}$. This provides sufficient repulsion coming from the three-body term to preclude any pathological solutions. Nevertheless, without the self-interaction energy term the theory possesses an unphysical behaviour: forcing two monomers very close to each other produces a rather weak repulsion of this pair from all very distant monomers. This repulsion comes from the three-body interaction and it is dominant at no matter how strong two-body attraction between monomers.

This effect comes into play only for sufficiently large negative $u^{(2)}$. In particular, it leads to a somewhat more convex than expected shape of the D_k function for the globule of a flexible homopolymer. Nevertheless, the kinetics of folding remains little affected by this deficiency. Adding the self-interaction energy term improves the situation and results in a flat shape of D_k (see Ref. 22 for more detail). For a stiff homopolymer there are even more pronounced problems associated with the pathological three-body repulsion in the absence of \mathcal{E}_{si} . So, from Fig. 4 of Ref. 3 one can see that there the size of the spherical globule was larger than that of the toroidal globule in the vicinity of the transition. Including the \mathcal{E}_{si} term reverses this situation as we shall see below. It also lowers the depths of the additional local free energy minima corresponding to phases such as T' and T'' in Fig. 6 of Ref. 3. Finally, the inclusion of the \mathcal{E}_{si} term leads to a better agreement with various results from Monte Carlo simulations for flexible and stiff homopolymers.

¹ L. Harnau, R.G. Winkler, and P. Reineker, *J. Chem. Phys.* **102** (19), 7750 (1995).

² F. Ganazzoli, R. La Ferla, and G. Allegra, *Macromolecules* **28** (15), 5285 (1995).

³ Yu. A. Kuznetsov, E. G. Timoshenko, and K. A. Dawson, *J. Chem. Phys.* **105** (16), 7116 (1996).

⁴ H. Isambert and A.C. Maggs, *Macromolecules* **29**, 1036 (1996).

⁵ V. V. Vasilevskaya, A. R. Khokhlov, S. Kidoaki, and K. Yoshikawa, *Biopolymers* **41**, 51 (1997).

⁶ J. P. K. Doye, R. P. Sear, and D. Frenkel, *J. Chem. Phys.* **108** (5), 2134 (1998).

⁷ A. Byrne, E. G. Timoshenko, and K. A. Dawson, *Il Nuovo Cimento*, **20D (12bis)** 2285 (1998).

⁸ V.A. Ivanov, W. Paul, and K. Binder, *J. Chem. Phys.* **109** (13), 5659 (1998).

⁹ P. Flory, *Principles of Polymer Chemistry* (Cornell University Press, Ithaca, NY, 1971); P. G. de Gennes, *Scaling Concepts in Polymer Physics* (Cornell University Press, Ithaca, NY, 3rd printing, 1988); M. Doi and S. F. Edwards, *The Theory of Polymer Dynamics* (Oxford Science, New York, 1989); A. Yu. Grosberg and A. R. Khokhlov, *Statistical Physics of Macromolecules* (AIP, NY, 1994).

¹⁰ J. des Cloizeaux and G. Jannink, *Polymers in Solution* (Clarendon Press, Oxford, 1990)

¹¹ E. G. Timoshenko, Yu. A. Kuznetsov, and K. A. Dawson, *J. Chem. Phys.* **102** (4), 1816 (1995).

- ¹² Yu. A. Kuznetsov, E. G. Timoshenko, and K. A. Dawson, *J. Chem. Phys.* **104** (9), 3338 (1996).
- ¹³ H. Orland and E. Pitard, *Europhys. Lett.* **41** (4), 467 (1998).
- ¹⁴ L.S. Lerman, *Proc. Natl. Acad. Sci. USA* **68**, 1886 (1971); U.K. Laemmli, *Proc. Natl. Acad. Sci. USA* **72**, 4288 (1975); Yu.M. Evdokimov *et al.*, *Nucl. Acids Res.* **3**, 2353 (1976); G.E. Plum, P.G. Arscott, and V.A. Bloomfield, *Biopolymers* **30**, 631 (1990); V.V. Vasilevskaya, A.R. Khokhlov Y. Matsuzawa, and K. Yoshikawa, *J. Chem. Phys.* **102**, 6595 (1995).
- ¹⁵ V.A. Bloomfield, *Biopolymers* **31**, 1471 (1991); J. Ubbink and T. Odijk, *Biophys. J.* **68**, 54 (1995); *ibid Europhys. Lett.* **33** (5), 353 (1996); N.V. Hud, K.H. Downing, and R. Balhorn, *Proc. Natl. Acad. Sci. USA* **92**, 3581 (1995).
- ¹⁶ A.Yu. Grosberg, *Biophysics* **24**, 30 (1979); A.Yu. Grosberg and A.R. Khokhlov, *Adv. Polym. Sci.* **41**, 53 (1981).
- ¹⁷ E. G. Timoshenko, Yu. A. Kuznetsov, and K. A. Dawson, *Phys. Rev. E* **57** (6), 6801 (1998).
- ¹⁸ Yu. A. Kuznetsov, E. G. Timoshenko, and K. A. Dawson. *J. Chem. Phys.* **103** (11), 4807 (1995).
- ¹⁹ Yu. A. Kuznetsov, E. G. Timoshenko, and K. A. Dawson. *J. Chem. Phys.* **104** (1), 336 (1996).
- ²⁰ O. Kratky and G. Porod, *Rec. Trav. Chim.* **68**, 1106 (1949).
- ²¹ R.A. Harris and J.E. Hearst, *J. Chem. Phys.* **44**, 2595 (1966).
- ²² Yu. A. Kuznetsov and E. G. Timoshenko, *Il Nuovo Cimento*, **20D (12bis)** 2265 (1998).
- ²³ See e.g. Sec. 2.2, Chap. 14 in Ref. 10 and Ref. 27.
- ²⁴ G. Allegra and F. Ganazzoli, *Adv. Chem. Phys.* **75**, 265 (J. Prigogine, S.A. Rice (Eds.), J. Wiley, 1989).
- ²⁵ E.G. Timoshenko, unpublished (1999).
- ²⁶ We should emphasise here that the order of a transition is defined by us according to how the main free energy minimum evolves upon a quasistatic movement in the parameter space. Such a definition is perfectly well justified even for finite-size systems, while the behaviour of some observables may appear fairly smooth in both cases due to finite size effects. This mean-field definition of the transition order manifests itself kinetically in the existence of a nucleation lag for discontinuous transitions. Unfortunately, in a computer simulation the determination of the order of transitions and even more so of the full phase diagram requires an enormous labour⁸. Practically, the boundary of a first order transition we determine here by the condition of equality of the free energy values on both of the competing minima, i.e. $\mathcal{A}_1 = \mathcal{A}_2$. For a second order transition there is a finite transition width involved and so, to be precise, we determine the transition point as the point of the maximal change of a corresponding order parameter X (R_g^2 in our case), i.e. $dX/dT = 0$.
- ²⁷ P.G. de Gennes, *J. Physique Lett.* **36**, L-55 (1975).
- ²⁸ E. G. Timoshenko, Yu. A. Kuznetsov, and K. A. Dawson, *Phys. Rev. E* **53** (4), 3886 (1996).

APPENDIX: FIGURE CAPTIONS

FIG. 1. Plot of the mean squared radius of gyration, R_g^2 , vs the second virial coefficient, $u^{(2)}$, upon a quasistatic change of the latter for ring homopolymer with $N = 100$. The solid line (diamonds) corresponds to the value of the stiffness parameter $\lambda = 5$, for which the collapse transition is second order. The dashed lines correspond to $\lambda = 25$ and are obtained by going from positive values of $u^{(2)}$ to negative (pluses) and backwards (quadrangles). Here labels (C), (G), and (T5)-(T7) correspond to the coil, the globule and various toroidal states respectively.

FIG. 2. Plot of the mean squared distances between monomers, D_k , vs the chain index, k , for various conformational states of the homopolymer. In Fig. 2a lines denoted by diamonds and pluses correspond to the coil ($u^{(2)} = 0$) and the globule ($u^{(2)} = -30$) for $\lambda = 25$. The solid line corresponds to the globule of flexible homopolymer ($\lambda = 0$ and $u^{(2)} = -25$). In Fig. 2b lines denoted by diamonds, pluses, and quadrangles correspond to the toroidal states with the winding number $\mathcal{N}_w = 5, 6$ and 7 ($\lambda = 25$, $u^{(2)} = -13, -17$ and -25) respectively.

FIG. 3. Plot of the mean squared radius of gyration, R_g^2 , vs the stiffness parameter, λ . Lines denoted by diamonds, pluses and quadrangles (from top to bottom) correspond to $u^{(2)} = -17, -20$ and -25 respectively.

FIG. 4. Phase diagram of the stiff homopolymer in terms of the stiffness parameter, λ , and the second virial coefficient, $u^{(2)}$ for $N = 100$. Here (C) denotes the transition curve between the coil and globular phases, and curves (C') and (C'') are the metastability boundaries of that transition. Labels (T5)-(T7) correspond to toroidal states with the winding number $\mathcal{N}_w = 5, 6$ and 7 respectively. The metastability boundaries of these transitions are not depicted.

FIG. 5. Snapshots of typical equilibrium conformations of a homopolymer with the degree of polymerisation $N = 100$ from the off-lattice Monte Carlo simulation. Figures (a)-(d) correspond to the coil ($V_0 = 0$, $\lambda = 5$), the globule of a semi-flexible homopolymer ($V_0 = 5$, $\lambda = 5$), the globule of the flexible homopolymer ($V_0 = 5$, $\lambda = 0$), and the toroidal globule ($V_0 = 5$, $\lambda = 15$).

FIG. 6. Snapshots of typical conformations of a stiff ($\lambda = 10$) homopolymer with $N = 100$ during kinetics after the quench from $V_0 = 0$ to $V_0 = 5$. Figures (a)-(c) correspond to the following moments in time: $t = 1.4 \cdot 10^6$ MCS, $t = 1.6 \cdot 10^6$ MCS, and $t = 10^7$ MCS. Here and in Fig. 7 the maximal attempted coordinate variance is $\Delta = 0.08$.

FIG. 7. Snapshots of typical conformations of a semi-flexible ($\lambda = 5$) homopolymer with the degree of polymerisation $N = 100$ during kinetics after the same quench as in Fig. 6. Figures (a)-(d) correspond to the following moments in time: $t = 350,000$ MCS, $t = 800,000$ MCS, $t = 10^6$ MCS, and $t = 5 \cdot 10^6$ MCS.

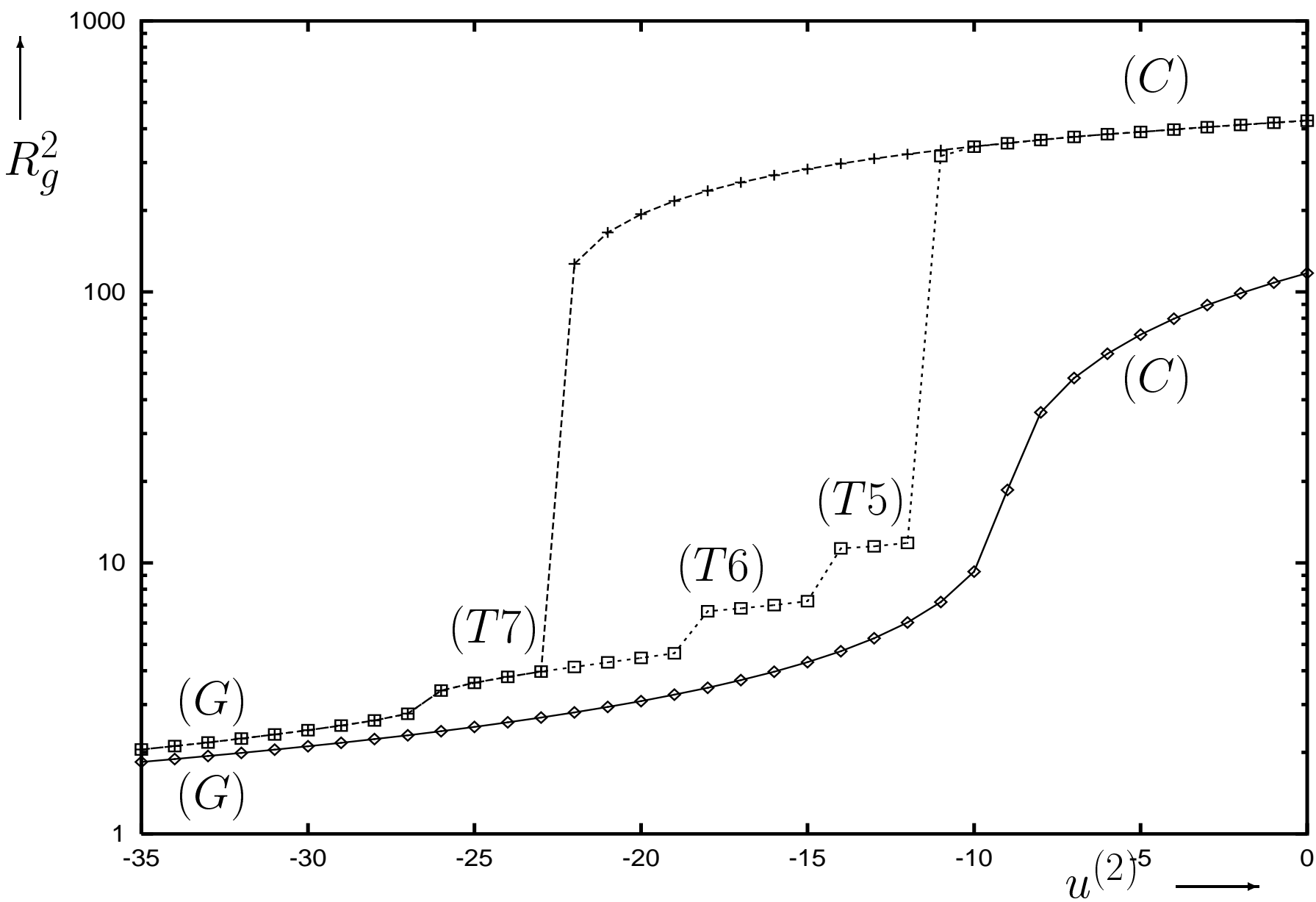


Fig. 1

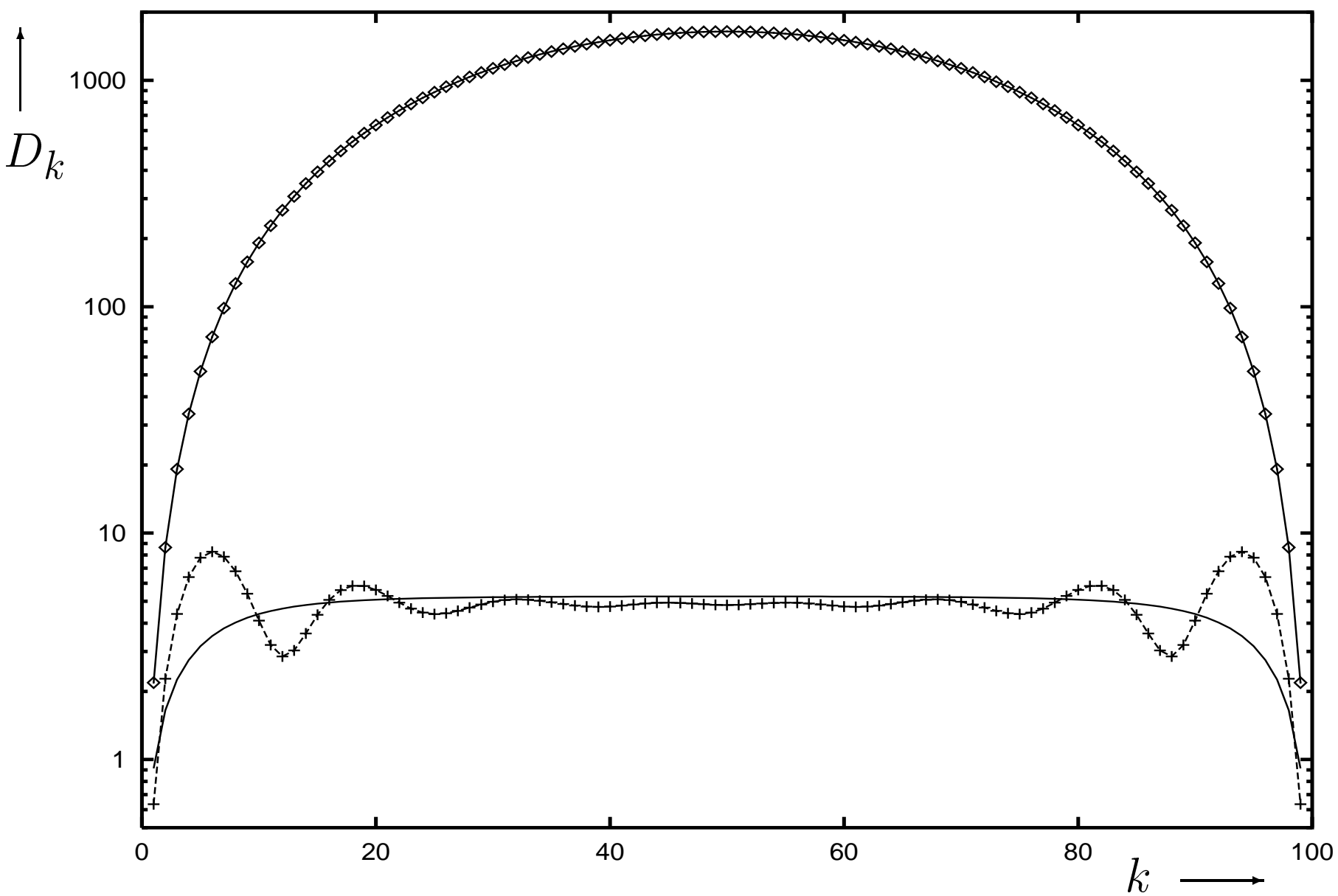


Fig. 2a

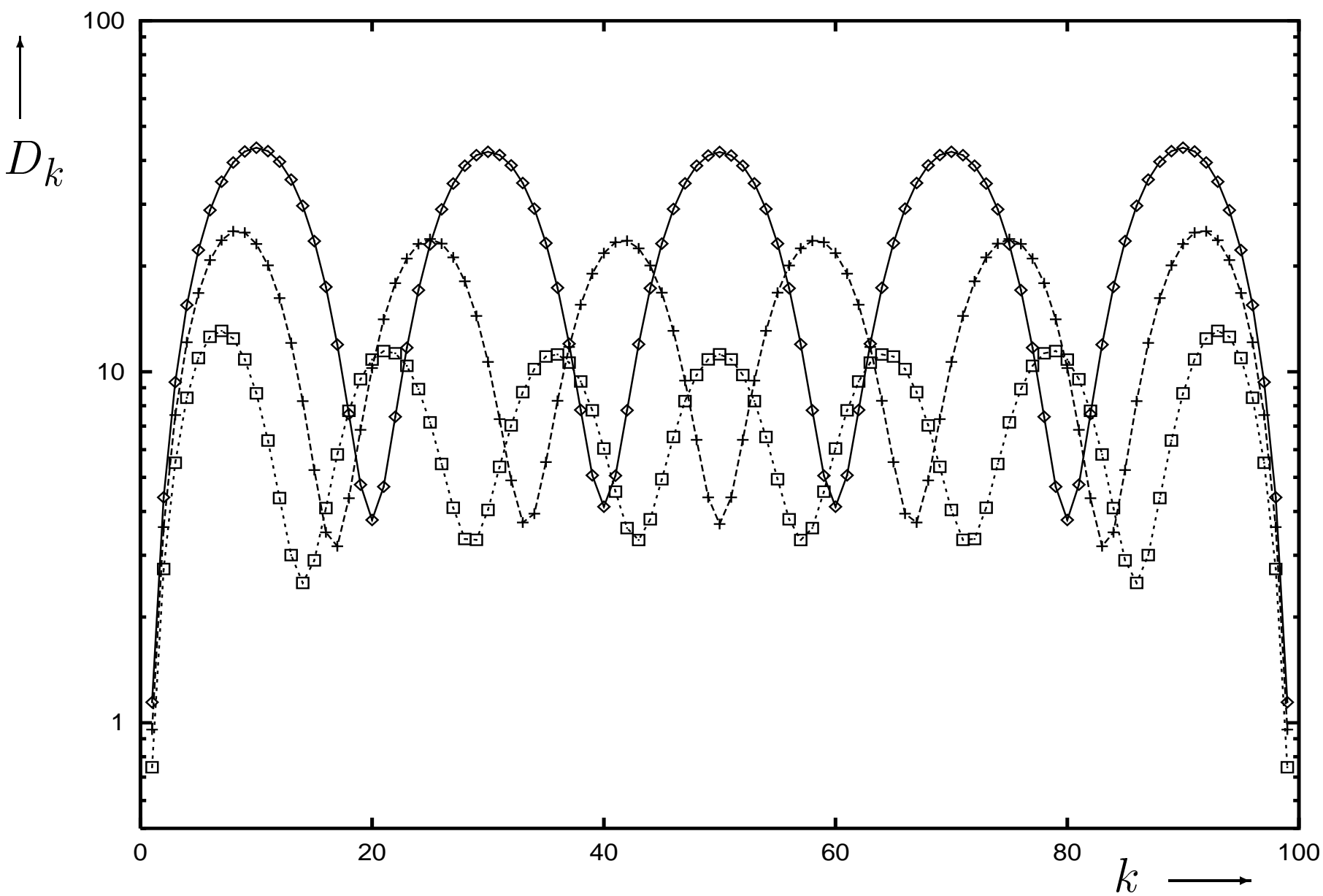


Fig. 2b

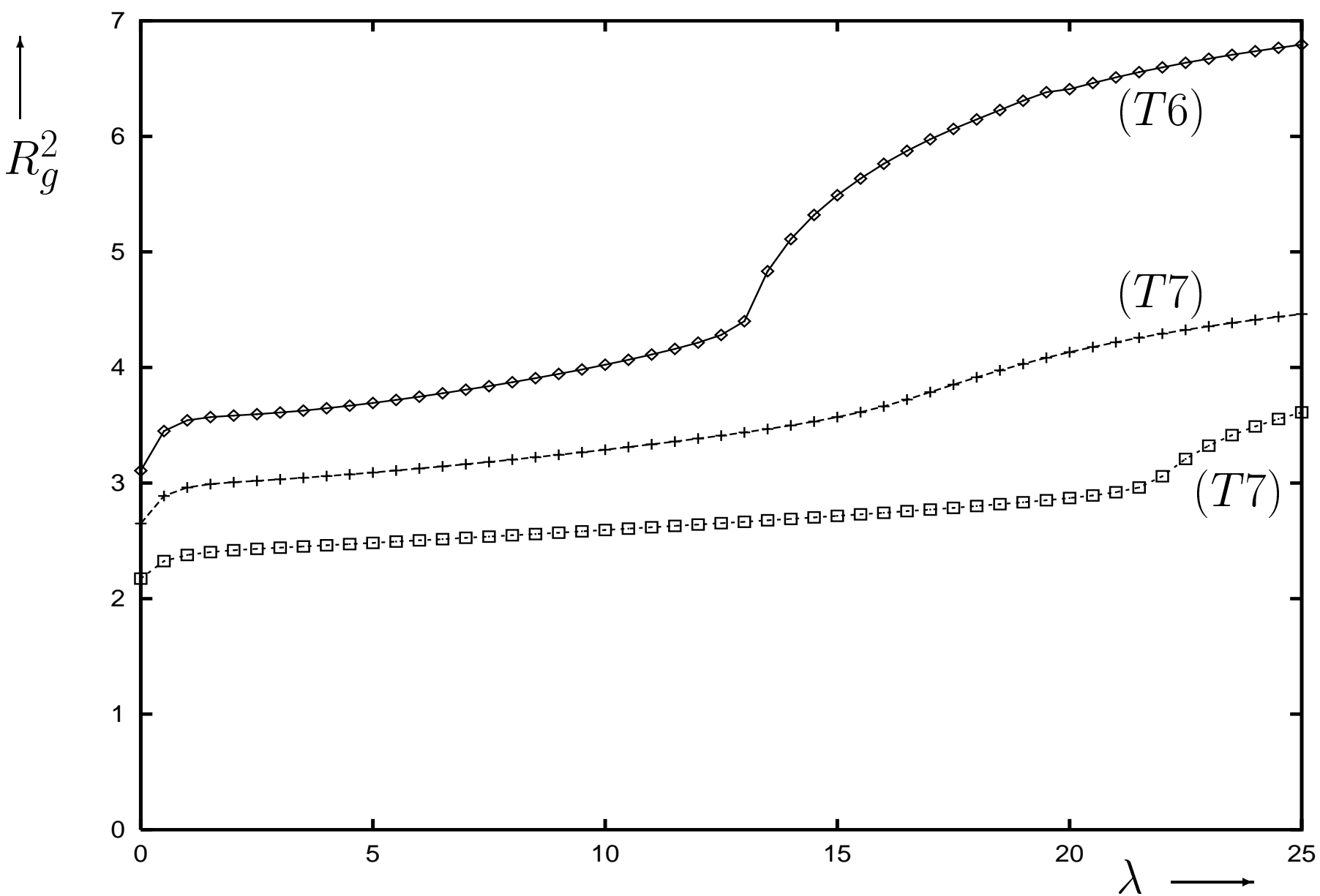


Fig. 3

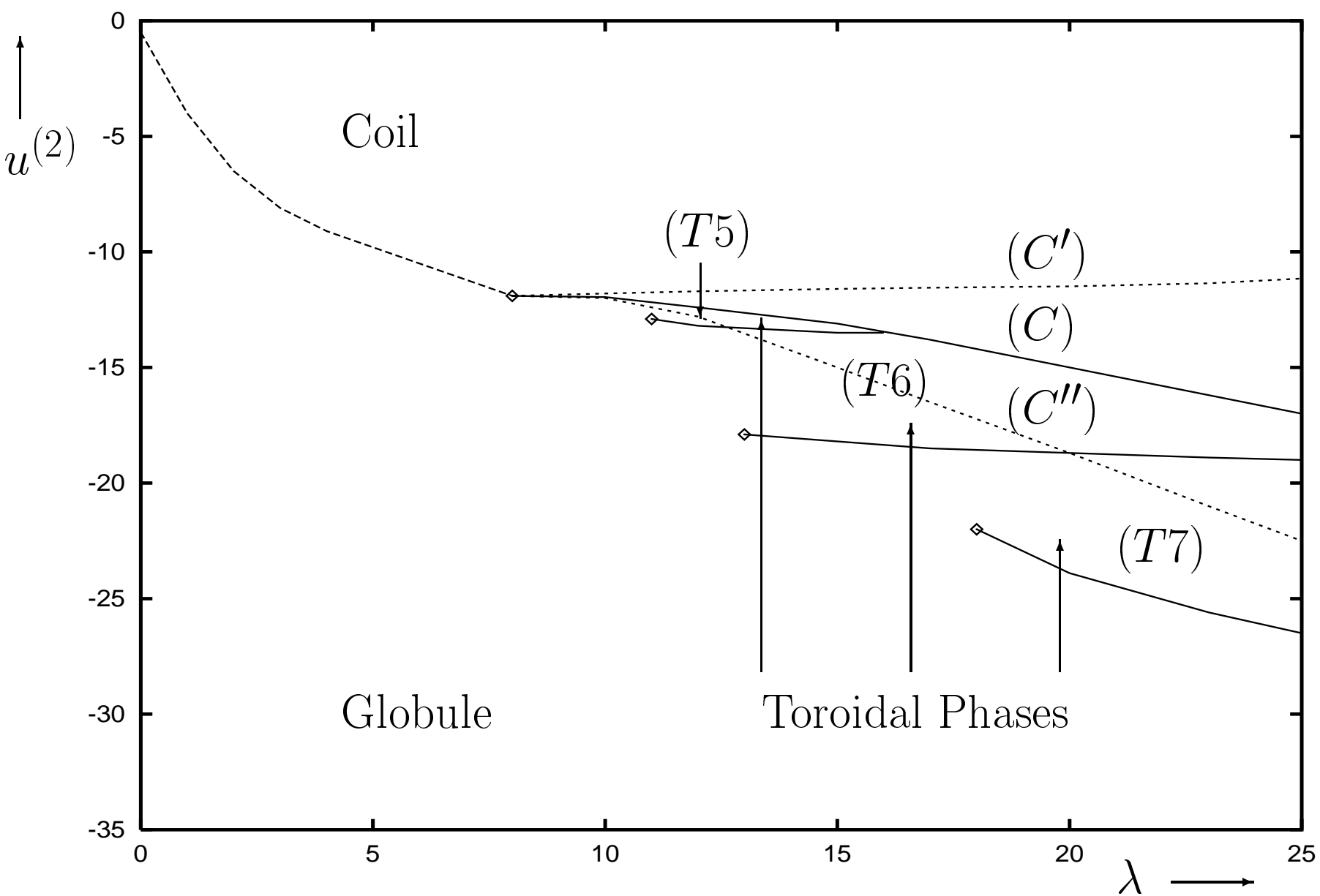


Fig. 4

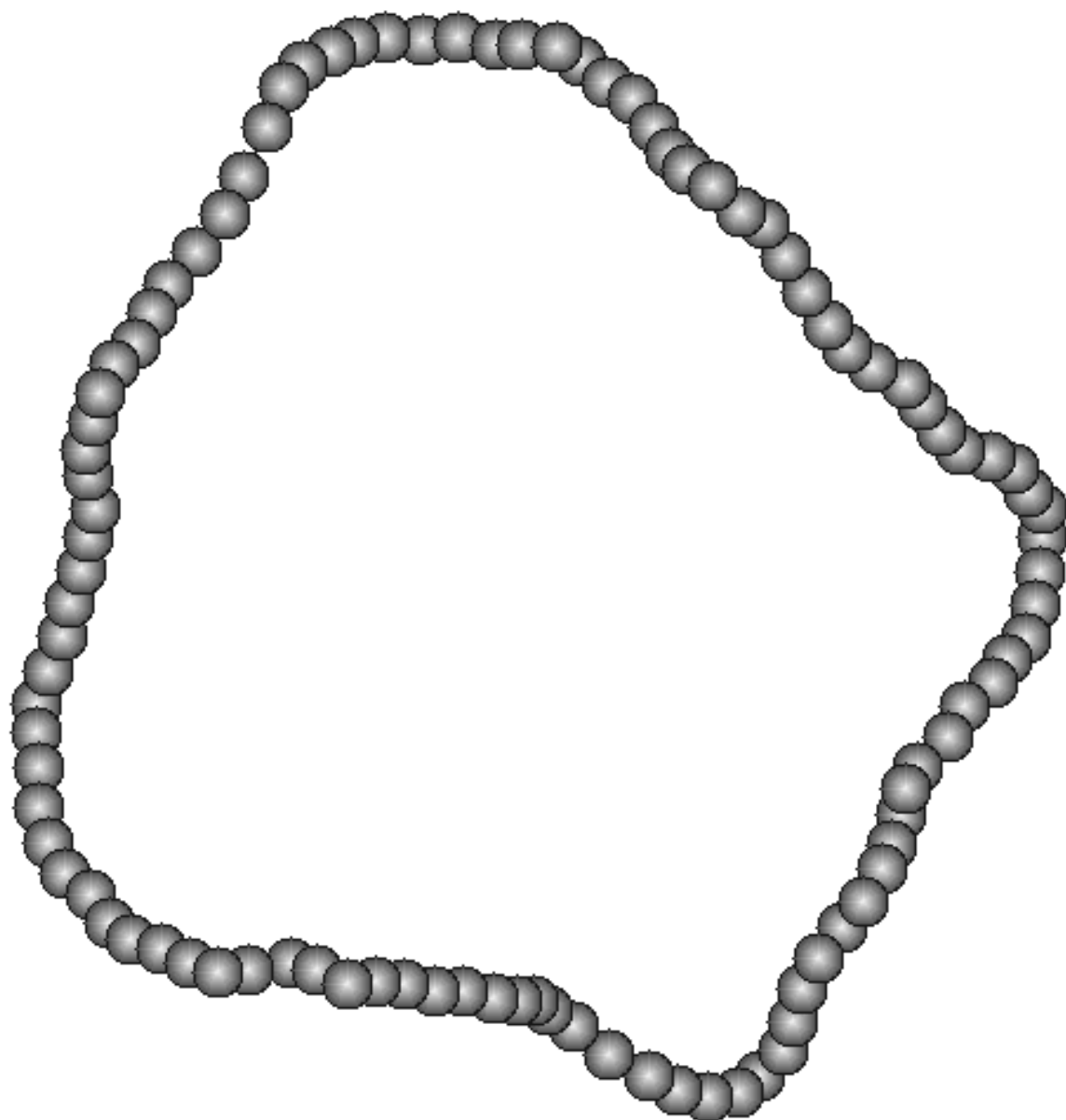


Fig. 5a

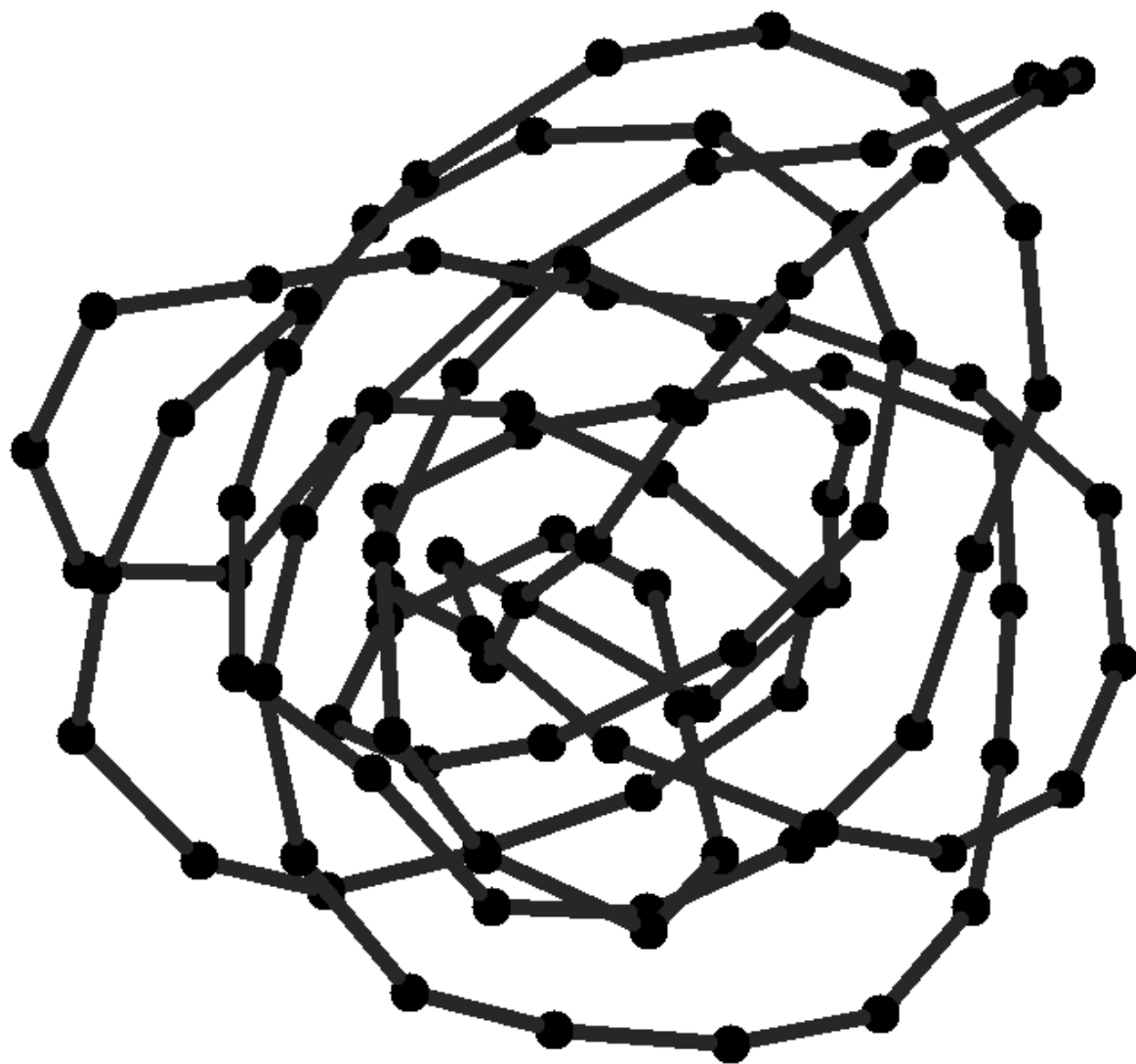


Fig. 5b

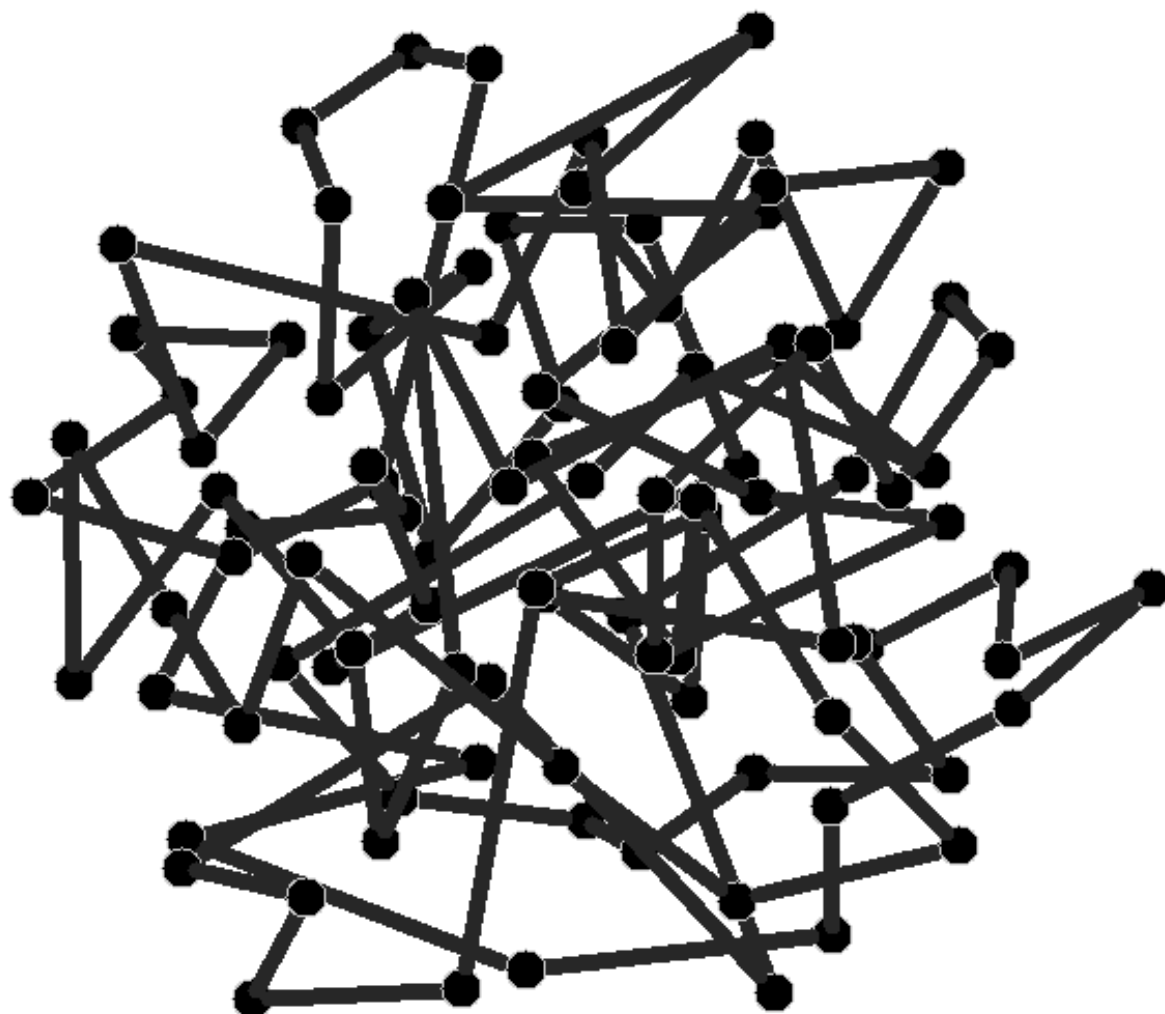


Fig. 5c

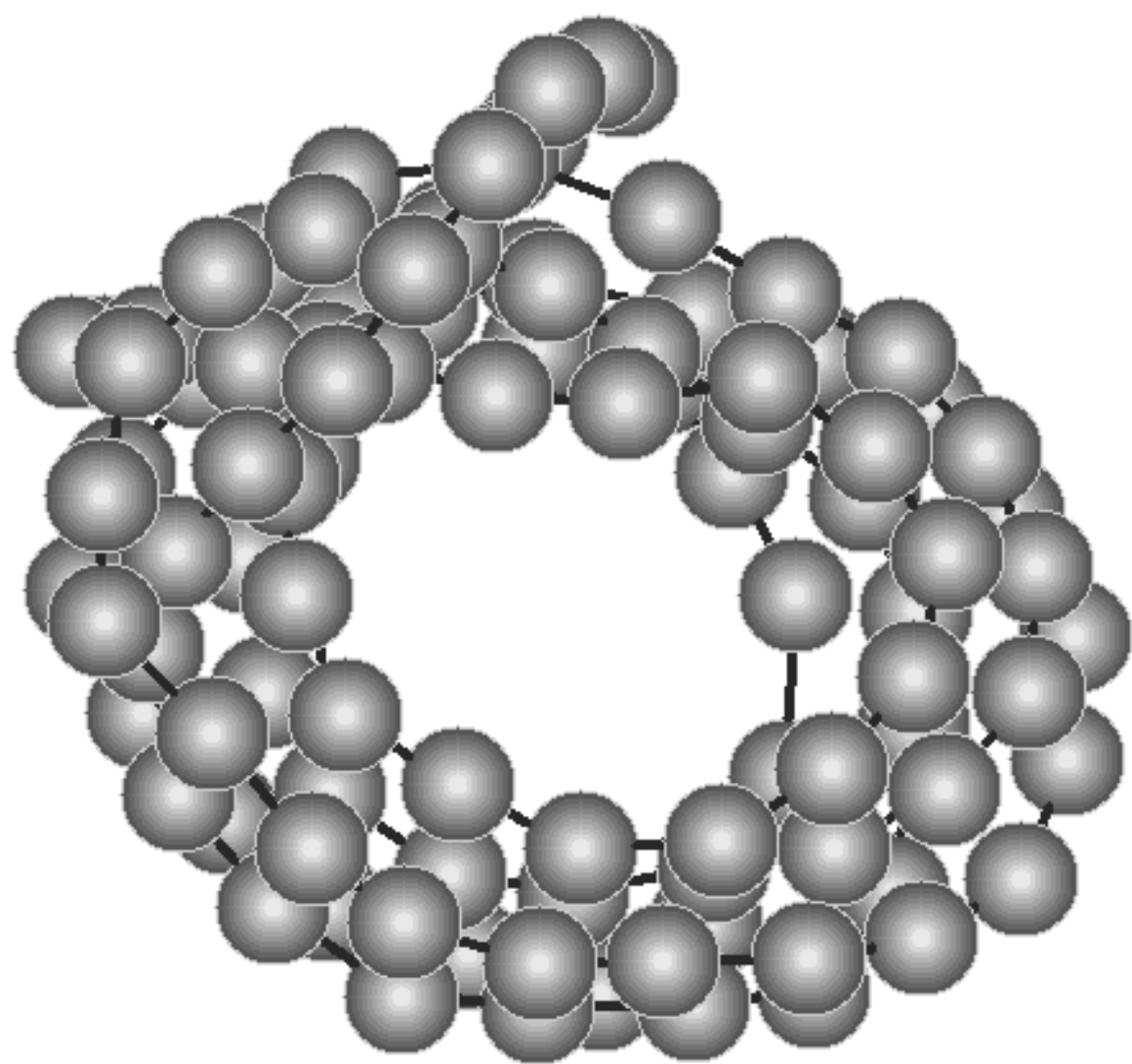


Fig. 5d



Fig. 6a



Fig. 6b



Fig. 6c

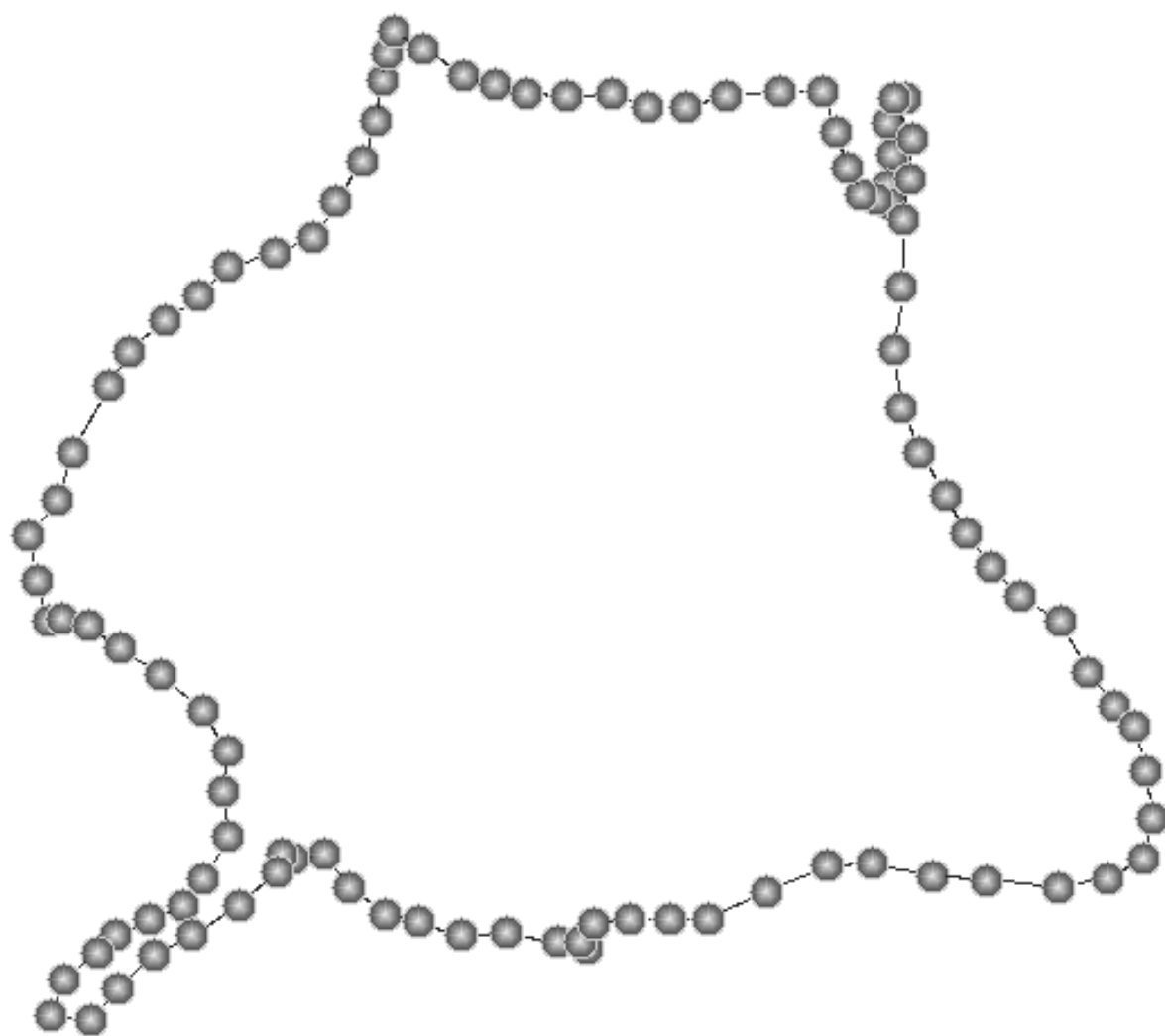


Fig. 7a



Fig. 7b

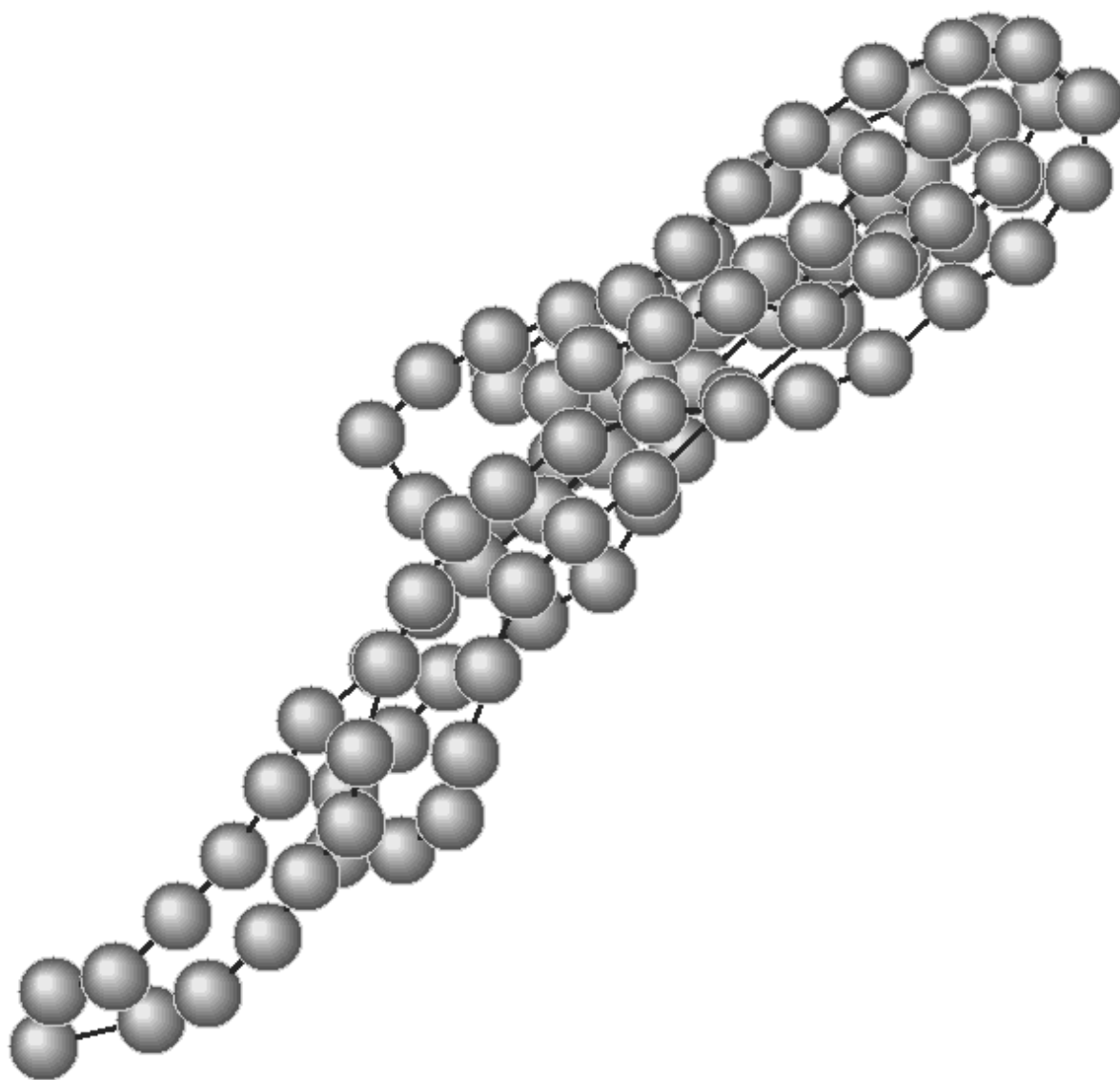


Fig. 7c

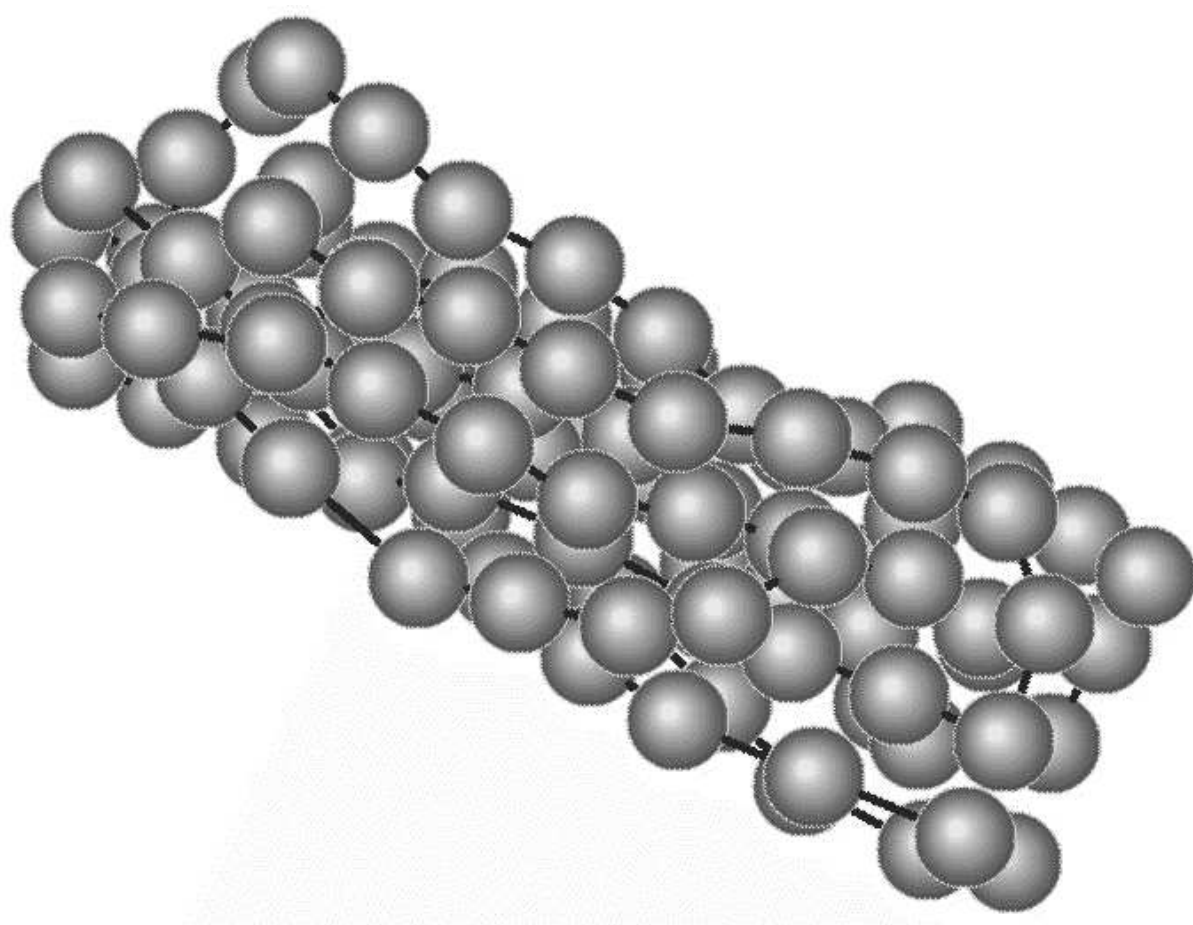


Fig. 7d